High-pressure thermal expansion, bulk modulus, and phonon structure of diamond

Jianjun Xie and S. P. Chen
Theoretical Division, Los Alamos National Laboratory, Los Alamos, New Mexico 87545

J. S. Tse
Steacie Institute for Molecular Science, National Research Council of Canada, Ottawa, Ontario, Canada K1A 0R6

Stefano de Gironcoli and Stefano Baroni
Scuola Internazionale Superiore di Studi Avanzati (SISSA) and Istituto Nazionale per la Fisica della Materia (INFM), via Beirut 2-4, I-34014 Trieste, Italy

(Received 9 March 1999; revised manuscript received 21 May 1999)

The thermodynamic properties of diamond at high pressures (up to 1000 GPa) have been investigated using the *ab initio* pseudopotential plane wave method and the density-functional perturbation theory. The *P-V-T* equation of states has been calculated from the Helmholtz free energy of the crystal in the quasiharmonic approximation. The pressure dependence of the equilibrium lattice constant, bulk modulus, mode Grüneisen parameters, and phonon structures has been presented. Some interesting dynamical features of diamond have been found at high pressures: (a) The thermal expansion coefficient decreases with the increase of pressure. At ultrahigh pressure ($\geqslant$700 GPa), diamond exhibits a negative thermal expansion coefficient at low temperatures. (b) The phonon frequency at X_4 and L_3' gradually goes higher than that of X_1 and L_2', respectively. (c) The unusual overbending of the uppermost phonon dispersion curves near Γ_{25}' decreases with the increase of pressure. Such overbending results in a maximum in the phonon density of states, which has been invoked in the previous study [Phys. Rev. B **48**, 3164 (1993)] to explain the famous sharp peak in the two-phonon Raman spectrum of diamond. Our present results predict that this sharp peak near the high-frequency cutoff will decrease with the pressure. [S0163-1829(99)03137-9]

I. INTRODUCTION

Nowadays, diamond-anvil-cell (DAC) technique is widely used as a powerful tool for generating high pressures in the laboratory.[1] The static high pressure obtained with DAC has been achieved up to 560 GPa.[2] Theoretical estimates of the stability limits of diamond under hydrostatic pressure have set an upper limit of 1110 GPa.[3] Other structures are predicted to be energetically favored when the pressure is even higher. A lot of studies[3–7] have been carried out on the possible phase transitions of diamond at ultrahigh pressures. However, there are comparatively fewer studies on the pressure dependence of the thermodynamic properties of diamond. This is in fact extremely important for accurate high pressure measurement, because not only the volume of the measured material but also the diamond itself changes with the pressure, especially when the pressure reaches hundreds of GPa. Such changes of diamond must be included in order to get an accurate *P-V-T* relationship, i.e., the equation of state of the measured material.

It has been known that diamond exhibits different thermal expansion behavior from other group-IV semiconductors such as Si and Ge at ambient pressure.[8–10] The characteristic negative behavior of Si and Ge in the low-temperature limit does not appear in diamond. Furthermore, the phonon dispersion curves of diamond are also quite unusual. The typical flatness of the transverse acoustic branches in large regions close to the boundaries of the Brillouin zone (BZ), which characterizes the other group-IV semiconductors, is completely lacking in diamond. The uppermost phonon branches of diamond overbend near Γ_{25}' point. Such noteworthy overbending is explained as the origin of the famous sharp peak near the high-frequency cutoff in the two-phonon Raman spectrum of diamond.[11]

All these facts motivate us to carry out a high pressure study on the above properties of diamond. In the present work, we have calculated the equation of state of diamond from the free energy of the crystal which consists of a *static* electronic contribution and a *dynamical* phonon contribution. In the quasiharmonic approximation, the latter nowadays can be conveniently calculated by using the density-functional perturbation theory (DFPT).[12] The thermal expansion coefficient, bulk modulus as well as the phonon structures of diamond are then calculated at different pressures and temperatures. The range of hydrostatic pressure considered here is up to 1000 GPa which is below the theoretical limit of phase transition of diamond. We have found that the thermal expansion coefficient decreases with pressure at a given temperature. When the pressure reaches 700 GPa, diamond also exhibits negative thermal expansion coefficient at low temperatures, similar to other group-IV semiconductors. The bulk modulus increases (decreases) with the increasing of pressure (temperature). The effect of pressure on the bulk modulus is much more significant than that of temperature. The overbending of the uppermost phonon branches near Γ_{25}' point gradually disappears with the increase of the imposing pressure. The phonon structure is significantly modified as the pressure increases.

The paper is organized as follows. In Sec. II, we briefly outline our computational framework, as well as some defi-

nitions concerning the physical quantities we have investigated. The results of our calculations are then presented and discussed in Sec. III. Finally, in Sec. IV we give our conclusions.

II. COMPUTATIONAL DETAILS

The free energy of a crystal can be expressed in the quasiharmonic approximation[13] as

$$F(V,T)=E(V)+F_{\mathrm{vib}}(\omega,T)$$
$$\equiv E(V)+k_{\mathrm{B}}T\sum_{\mathbf{q}}\sum_{j}\ln\left\{2\sinh\left(\frac{\hbar\omega_j(\mathbf{q})}{2k_{\mathrm{B}}T}\right)\right\}, \tag{2.1}$$

where E is the *static* contribution to the internal energy—which is easily accessible to standard density-functional theory (DFT) calculations—F_{vib} represents the vibrational contribution to the free energy, and $\omega_j(\mathbf{q})$ is the frequency of the jth phonon mode at wave vector $\mathbf{q}$ in the Brillouin zone (BZ). The lattice dependence of frequency $\omega_j(\mathbf{q})$ is calculated by the parameter-free DFPT.[12] Here the anharmonicity appears not only in the *static* internal energy $E(V)$ which includes all the anharmonic terms of the interatomic potential, but also in the lattice parameter dependence of the phonon frequency ω. The atomic motion is then approximated by a system of uncoupled normal vibrations but with different equilibrium positions and vibration frequencies. Calculations based on various semiempirical models[8,14,15] as well as on first-principles methods[10,16–18] demonstrate that the quasiharmonic approximation provides a reasonable description of the dynamic properties of many bulk materials below the melting point.

The equation of state can then be written in the form

$$p(V,T)=-\frac{\partial E}{\partial V}-\frac{\partial F_{\mathrm{vib}}}{\partial V}$$
$$=-\frac{\partial E}{\partial V}+\frac{1}{V}\sum_{\mathbf{q}}\sum_{j}\gamma_j(\mathbf{q})\mathcal{E}[\omega_j(\mathbf{q})], \tag{2.2}$$

where $\gamma_j(\mathbf{q})$ is the Grüneisen parameter corresponding to the $(\mathbf{q},j)$ phonon mode, defined as

$$\gamma_j(\mathbf{q})=-\frac{\partial\omega_j(\mathbf{q})}{\partial V}\frac{V}{\omega_j(\mathbf{q})}, \tag{2.3}$$

and $\mathcal{E}[\omega_j(\mathbf{q})]$ is the mean vibrational energy of the $(\mathbf{q},j)$ phonon given by

$$\mathcal{E}(\omega_j(\mathbf{q}))=\hbar\omega_j(\mathbf{q})\left[\frac{1}{2}+\frac{1}{\exp[\hbar\omega_j(\mathbf{q})/k_BT]-1}\right]. \tag{2.4}$$

Having the equation of state at hand, we can easily calculate the thermal expansion and the bulk modulus as a functional of temperature and pressure.[18]

The total energy is calculated by using separable norm-conserving Hamann-type pseudopotentials[19–21] together with a plane-wave basis set up to a kinetic-energy cutoff of 70 Ry. We noted that such a large kinetic energy cutoff is required to give well converged total energy and phonon frequencies of diamond due to the small cutoff radius needed in the calculations, especially at high pressures. The expression of the exchange-correlation energy in local-density approximation (LDA) is taken from Ref. 22. Sums over occupied electronic states are performed by the Monkhorst-Pack special-point technique,[23] using 10 $\mathbf{k}$ points in the irreducible wedge of BZ. Phonon frequencies are calculated on a $(4\times4\times4)$ regular mesh and Fourier-interpolated in between. This Fourier interpolation amounts to including real-space interatomic force constants up to the ninth shell of neighbors. Variation of the calculated phonon frequencies is less than 1% by further increasing the interaction distances, i.e., using a larger mesh. The phonon density of states (DOS) is calculated by using the linear tetrahedral method[24] and total of 560 special $\mathbf{q}$ points in the irreducible wedge of the BZ (corresponding to 2653 nonequivalent tetrahedra).

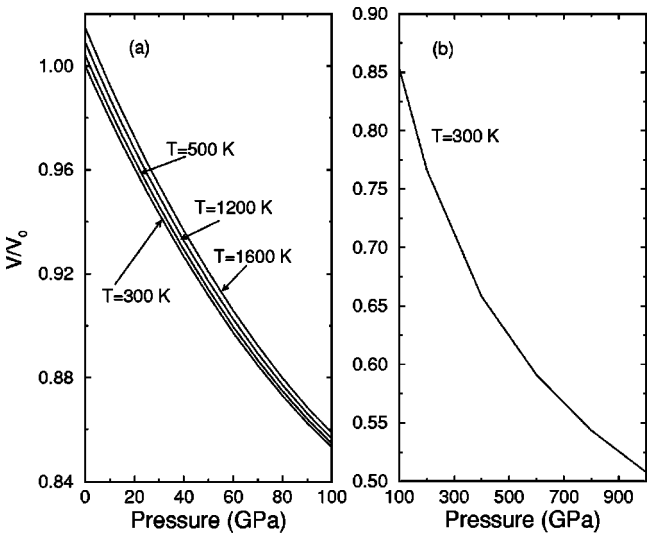

FIG. 1. Calculated P-V-T relationship of diamond for (a) $0 \leqslant P \leqslant 100$ GPa, (b) $100 \leqslant P \leqslant 1000$ GPa.

III. RESULTS

We first calculated the P-V-T equation of state of diamond according to Eq. (2.2). The results are shown in Fig. 1. V_0 is the equilibrium volume of the unit cell at $T=300$ K and zero pressure. The calculated value of V_0 is 44.391 Å^3,

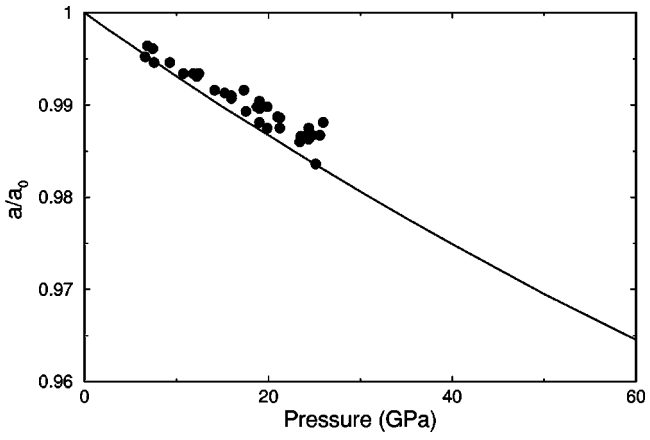

FIG. 2. Comparison of the calculated a/a_0 vs pressure (solid line) at $T=300$ K with the experimental results 26 (filled circles).

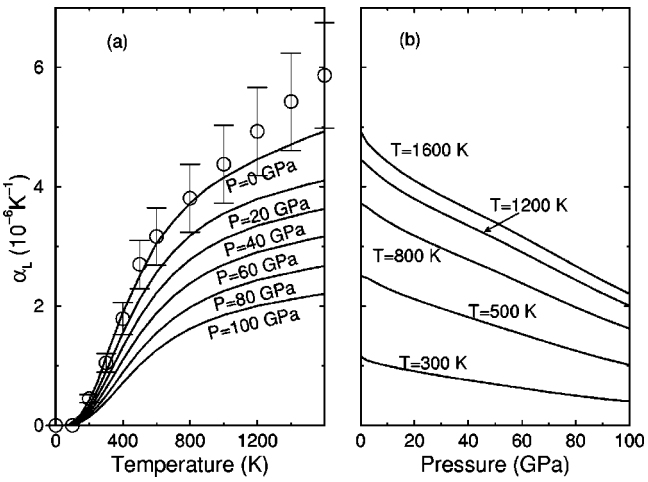

FIG. 3. Variation of the linear thermal expansion coefficient α_L with temperature (a) and pressure (b). The available experimental results are shown by circles including the error bar 27. The range of the pressure is from 0 to 100 GPa.

the corresponding lattice constant $a_0=3.541$ Å (here $V_0=a_0^3/4$, each unit cell has two carbon atoms), in good agreement with the experimental value of 3.567 Å at room temperature.[25] It can be seen that the volume of diamond decreases monotonically with pressure. At a given pressure, higher temperature gives a larger volume due to the thermal expansion [see Fig. 1(a)]. As pressure increases, the effect of thermal expansion becomes less significant. Figure 1(b) shows the P-V isotherm at the high pressure domain ($P \geqslant 100$ GPa) for $T=300$ K. We can see that at $P=300$ GPa, which is an achievable pressure in DAC, the equilibrium volume of diamond is 0.713 V_0. Such a change is apparently non-negligible in the ultrahigh pressure experiment using DAC technique. Figure 2 shows the comparison of the calculated a/a_0 vs pressure with the available experimental results[26] which were obtained by high-pressure x-ray techniques. In general, the theory agrees well with the experiment. The slight difference could be a result of the approximations used in the calculations, e.g., the local-density approximation. On the other hand, the experimental data themselves are rather scattered. If the experiments did not achieve a perfect uniform compression of the diamond sample, the uniaxial strain would lead to a slightly higher average of lattice constant, which may result in the overall larger value of the measured a/a_0 comparing with the theoretical results (see Fig. 2).

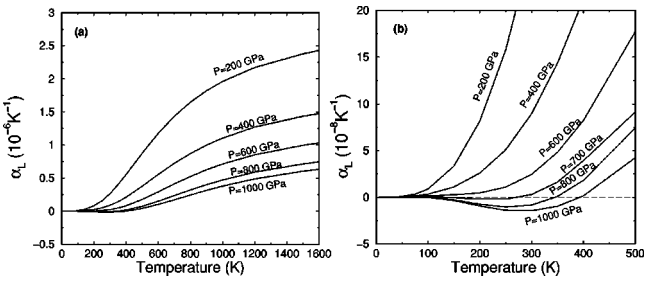

FIG. 4. Calculated linear thermal expansion coefficient α_L at high pressure range ($200 \geqslant P \geqslant 1000$ GPa). (a) $0 \leqslant T \leqslant 1600$ K, (b) $0 \leqslant T \leqslant 500$ K.

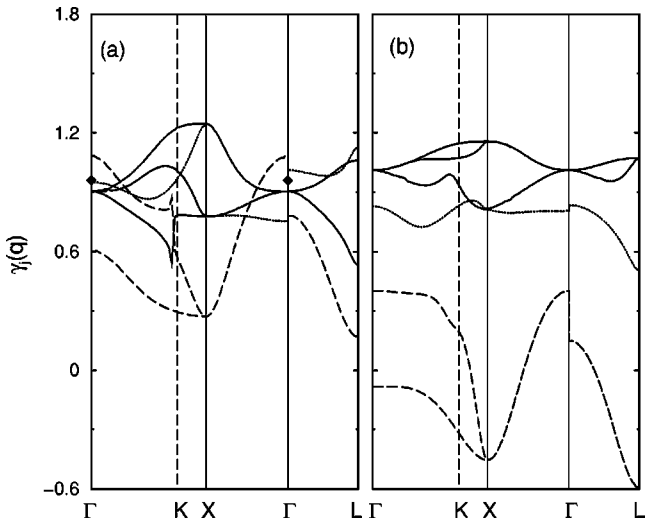

FIG. 5. Mode Grüneisen parameters for diamond at different pressure: (a) $P=0$ GPa, (b) $P=700$ GPa. Dashed lines correspond to transverse acoustic modes, dotted lines to longitudinal acoustic modes, and solid lines to optical modes. The experimental data 25 are denoted by diamonds.

The variation of the linear thermal expansion coefficient α_L of diamond with temperature and pressure is shown in Fig. 3. Here α_L is defined as

$$\alpha_L=\frac{1}{l_0}\frac{dl}{dT} \tag{3.1}$$

in order to compare with the experimental values[27] directly [circles in Fig. 3(a)]. l_0 is the equilibrium lattice constant at $T=300$ K. It can be seen that the theoretical results at zero pressure are in good agreement with the corresponding experimental data within the experimental error bar. No negative thermal expansion is found at the low temperature range which is in agreement with the previous theoretical calculations[8,10] and the experimental measurements.[9,27] When the pressure increases, the increase of α_L with temperature becomes smaller, especially at high temperature range. At a given temperature, α_L decreases monotonically with pressure [see Fig. 3(b)], which means the thermal expansion is suppressed by the pressure. This is easy to understand. At high pressure, the interaction between atoms becomes strong, which makes phonon frequency increase as the interatomic distance decreases. As the phonon frequency increases, the number of phonons excited at a given temperature decreases. The vibrational contribution to the free energy [$F_{\mathrm{vib}}(\omega,T)$] becomes less important than the static contribution [$E(V)$] at high pressure. The thermal expansion is thus less significant at high pressure.

We plotted the variation of the linear thermal expansion coefficient α_L with temperature at the high pressure domain ($P \geqslant 200$ GPa) in Fig. 4. We can see that α_L decreases continuously as the pressure increases. When the pressure is high enough, e.g., 700 GPa, the negative thermal expansion occurs at the low temperature range [see Fig. 4(b)]. This is an interesting phenomenon that has not been reported. Although the transition pressure of α_L is higher than the achievable pressures in DAC presently, other high-pressure techniques such as shock-wave method[28] may verify this.

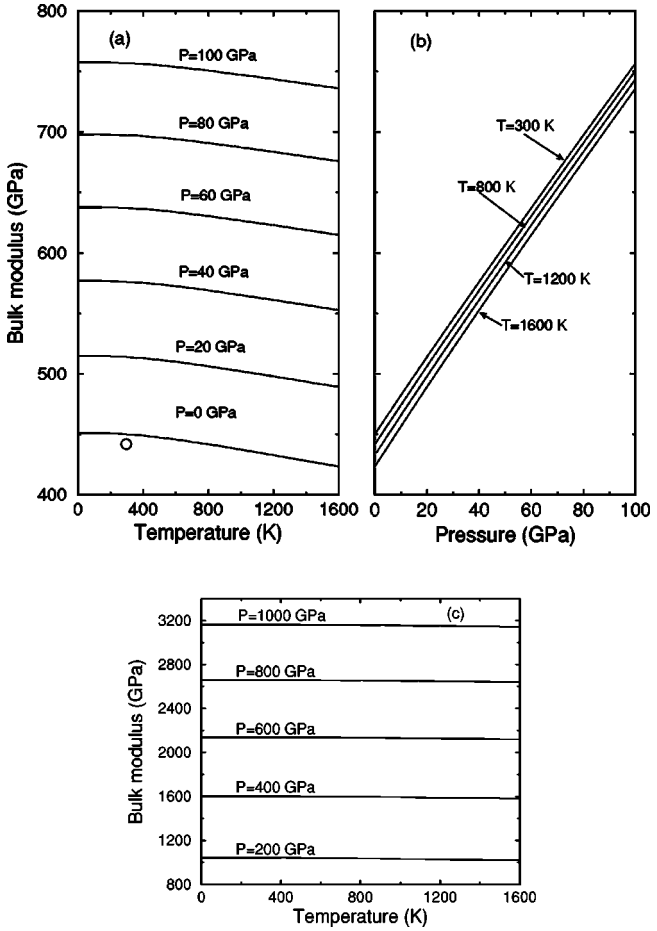

FIG. 6. Variation of the bulk modulus of diamond with temperature (a) and pressure (b) in the case of pressure below 100 GPa. The temperature dependence of bulk modulus for pressures between 200 GPa and 1000 GPa is shown in (c). The experimental result at 298 K and ambient pressure is denoted by circle (from Ref. 25).

In order to verify the origin of the interesting changes of the thermal expansion coefficient, we plotted the Grüneisen parameters $\gamma_j(\mathbf{q})$ at different pressures in Fig. 5. The available experimental data[25] are also displayed. It can be seen that at zero pressure, the Grüneisen parameters along all the branches are positive, therefore, no negative thermal expansion occurs. When the pressure reaches 700 GPa, strong negative Grüneisen parameters are found for the transverse acoustic (TA) branches especially near the BZ boundaries X and L which is quite similar to the case of Si at ambient pressure.[8] It is such negative Grüneisen parameters that result in the negative thermal expansion coefficient of diamond at high pressure. The transition of Grüneisen parameter from positive to negative value reflects the changes of the interatomic forces with external pressure in diamond. Analysis of the atomic vibrations at TA(X) and TA(L) shows the polarizations of these two modes are associated with pure bond-bending motion: the bonds between atoms are distorted by atomic motions perpendicular to the bonds. At low pressure, the angular force constants are dominant in diamond. These angular force constants favor positive Grüneisen parameter. When the pressure increases, the contribution of stretching force constants becomes significant and therefore the negative Grüneisen behavior occurs. Analysis of the force constants of silicon shows that the stretching force constants are dominant, that is why silicon has negative thermal expansion at ambient pressure.[8–10]

The unusual bonding strength of diamond makes it an extremely low compressibility material which is characterized by a very large bulk modulus. The calculated relationship of B-P-T is shown in Fig. 6. The corresponding experimental value of 443 GPa for $T=298$ K from Ref. 29 is also displayed in Fig. 6(a). At a fixed pressure P [Fig. 6(a)], B decreases with the increase of T. While, at a given temperature T [Fig. 6(b)], B increases nearly linearly with P. From the comparison of Figs. 6(a) and 6(b), we can see that the effect of pressure on B is much more significant than that of temperature. The B-P-T relationship of diamond in high pressure domain ($P \geqslant 200$ GPa) is shown in Fig. 6(c). The bulk modulus continuously increases with pressure, while the temperature dependence of B becomes much smaller at high pressures. This is because the bulk modulus is related to

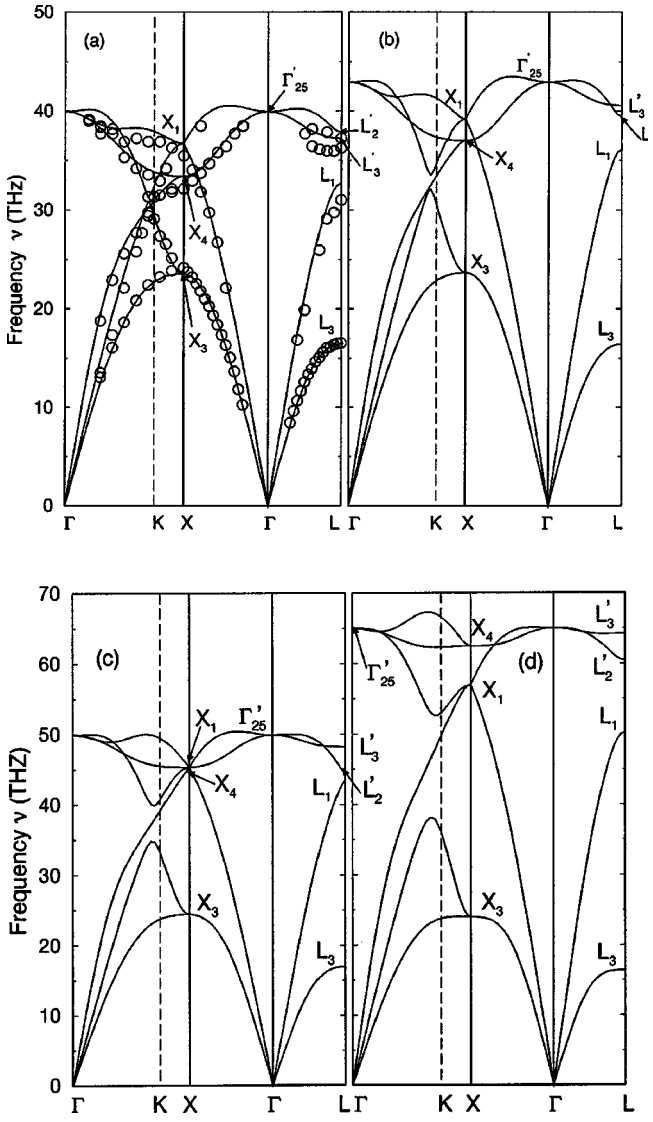

FIG. 7. Pressure dependence of the phonon dispersion curves of diamond at $T=300$ K. (a) $P=0$ GPa, (b) $P=50$ GPa, (c) $P=200$ GPa, (d) $P=600$ GPa. The experimental data obtained from inelastic neutron scattering (from Ref. 30 at room temperature).

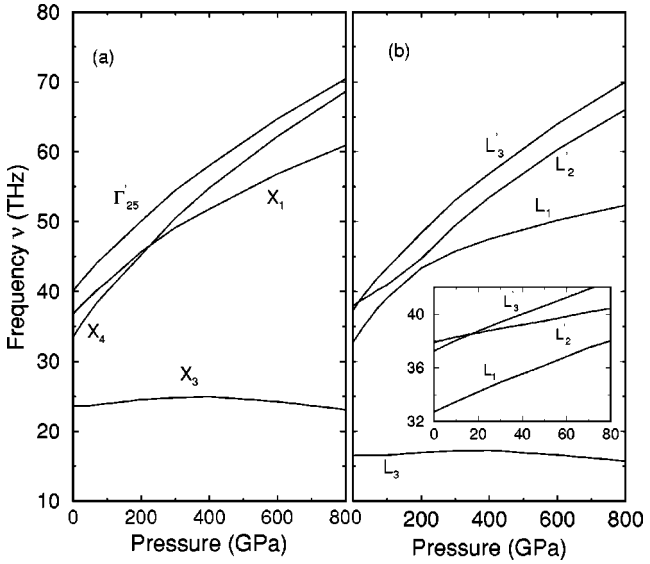

FIG. 8. Pressure dependence of the phonon frequency of diamond at (a) Γ and X and (b) L. The inset in (b) shows the details at low pressure range.

the volume derivative of pressure $[B=-V(\partial P/\partial V)_T]$. The vibrational contribution to P [see Eq. (2.2)] becomes less significant at high pressures since the number of the excited phonon modes decreases. While the static internal energy $E(V)$ increases drastically as the volume decreases (the pressure increases). The V-P isotherm (see Fig. 1) becomes flatter at high pressure which means the negative volume derivative of pressure $(-\partial P/\partial V)$ is getting larger. Therefore, at high pressure, diamond has larger bulk modulus.

Figure 7 shows the pressure dependence of the phonon dispersion curves of diamond along some high-symmetry lines in BZ . At zero pressure, the calculated phonon dispersion curves are in good agreement with the inelastic neutron scattering measurement.[30] As the pressure increases [see Fig. 7(b)], all the phonon branches move to higher frequency range accordingly. However, the increasing magnitude at different points in BZ is different. It can be seen that when $P=50$ GPa, the frequency at L_2' becomes lower than that of L_3'. The frequency difference between X_1 and X_4 becomes smaller than that of in Fig. 7(a). When pressure goes even higher [see Fig. 7(c) and (d)], X_1 and X_4 change position with each other. The frequency at X_4 becomes higher than that of X_1 in Fig. 7(d). The detailed variations of frequency at Γ, X, and L with pressure are shown in Fig. 8. It can be seen that phonon frequencies at Γ_{25}', X_1, X_4, L_3', L_2', and L_1 increases monotonically with pressure. While frequencies at X_3 and L_3 first increase then decrease as the pressure increases from zero to 800 GPa. Such decrease of frequency with pressure means that the Grüneisen parameters at these points will become negative. It is found from Fig. 8 that the pressure for the crossing point of L_2' and L_3' is 17 GPa; for the crossing point of X_1 and X_4 it is 230 GPa.

Figure 9 shows the pressure dependence of phonon density of states (DOS). When pressure increases from 0 to 100 GPa [Fig. 9(a)], all the peaks in DOS move to higher frequency range accordingly. When pressure is higher than 600 GPa, two DOS peaks in the low frequency range shift downwards which corresponds to the decrease of frequency of the acoustic modes at X_3 and L_3. Other peaks shift upwards continually. One interesting feature is that the DOS peak at the uppermost frequency cutoff (40.1 THz for zero pressure) decreases gradually with the increase of pressure [see Fig. 9(a)]. This peak originates from the overbending of the uppermost phonon dispersion curve near Γ_{25}' [see Fig.7(a)], which is completely absent in the phonon structure of other group-IV semiconductors. Early analysis[11] demonstrated that this peak in phonon DOS was the origin of the famous sharp peak in the second-order Raman spectra. The present calculation suggests that the sharp peak in the second-order Raman spectra will decrease when pressure is imposed on the diamond sample. It will be very interesting to verify this phenomenon by experiment since the origin of this Raman peak has been a longstanding controversy. Another DOS peak appears at the uppermost frequency cutoff when pressure is higher than 400 GPa. However, this peak does not come from the overbending of the uppermost phonon dispersion curve near Γ_{25}' but from the uplift of the optical branch between Γ_{25}' and X_4 [see Fig. 9(b)]. The overbending of the uppermost phonon dispersion curve near Γ_{25}' of diamond also originates from its unusual interatomic force constants, similar to the Grüneisen parameters. As stated before, the angular forces are much stronger in diamond than in silicon

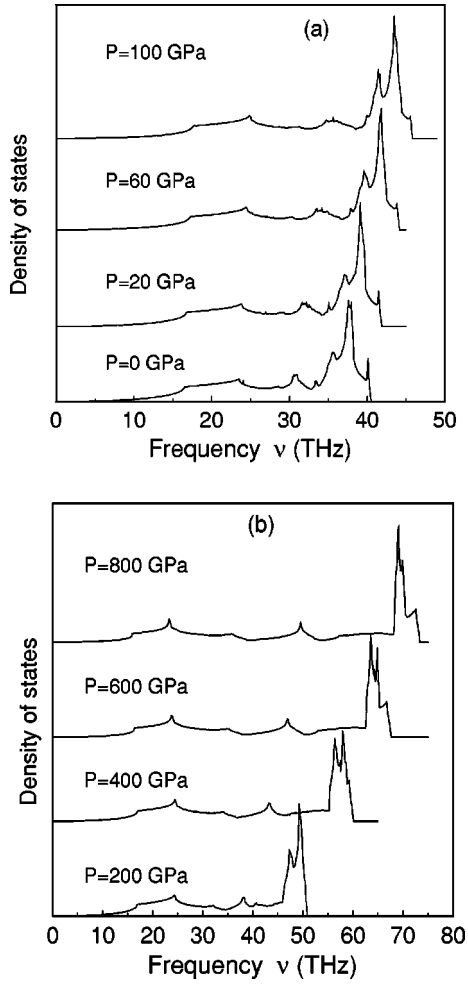

FIG. 9. Pressure dependence of the phonon density of states of diamond (a) $0 \leqslant P \leqslant 100$ GPa, (b) $200 \leqslant P \leqslant 800$ GPa.

at low pressure, which gives rise to the overbending of phonon structure of diamond. As pressure increases, the ratio of angular force constants to stretching force constants in diamond decreases, therefore the overbending of the phonon dispersion curve disappears gradually. The variation of the phonon structure with pressure (Fig. 7) also comes from these changes of the interatomic force constants.

IV. CONCLUSIONS

In the present paper, we have calculated the thermodynamic properties of diamond, such as P-V-T equation of state, thermal expansion coefficient, Grüneisen parameters, and bulk modulus at high hydrostatic pressures, using the quasiharmonic approximation within density-functional theory. The obtained results for the investigated thermodynamic quantities are in good agreement with the available experimental measurements. At ultrahigh pressure ($\geqslant$700 GPa), we find that diamond also exhibits negative thermal expansion coefficient at low temperatures. Furthermore, it is found the phonon structure of diamond is modified by imposing pressures. The phonon frequencies at X_4 and L_3' gradually go higher than that of X_1 and L_2', respectively. The unusual overbending of the diamond phonon dispersion curve near Γ_{25}' decreases with the increase of pressure, which suggests that the famous sharp peak in the second-order Raman spectra will decrease with pressure accordingly.

ACKNOWLEDGMENT

This work was supported by the U.S. Department of Energy under Contract No. W-7405-ENG-36.

[1] H.K. Mao and R.J. Hemley, Nature (London) **351**, 721 (1991).
[2] A.L. Ruoff, H. Luo, and Y.K. Vohra, J. Appl. Phys. **69**, 6413 (1991).
[3] S. Fahy and S.G. Louie, Phys. Rev. B **36**, 3373 (1986).
[4] M.T. Yin and M.L. Cohen, Phys. Rev. Lett. **50**, 2006 (1983).
[5] R. Biswas, R.M. Martin, R.J. Needs, and O.H. Nielsen, Phys. Rev. B **30**, 3210 (1984).
[6] S. Scandolo, G.L. Chiarotti, and E. Tosatti, Phys. Rev. B **53**, 5051 (1996).
[7] S. Serra, G. Benedek, M. Facchinetti, and L. Miglio, Phys. Rev. B **57**, 5661 (1998).
[8] C.H. Xu, C.Z. Wang, C.T. Chang, and K.M. Ho, Phys. Rev. B **43**, 5024 (1991).
[9] K. Haruna, H. Maeta, K. Ohashi, and T. Koike, Jpn. J. Appl. Phys. **31**, 2527 (1992).
[10] P. Pavone, K. Karch, O. Schütt, W. Windl, D. Strauch, P. Giannozzi, and S. Baroni, Phys. Rev. B **48**, 3156 (1993).
[11] W. Windl, P. Pavone, K. Karch, O. Schütt, D. Strauch, P. Giannozi, and S. Baroni, Phys. Rev. B **48**, 3164 (1993).
[12] S. Baroni, P. Giannozzi, and A. Testa, Phys. Rev. Lett. **58**, 1861 (1987); P. Giannozzi, S. de Gironcoli, P. Pavone, and S. Baroni, Phys. Rev. B **43**, 7231 (1991).
[13] R.E. Allen and F.W. de Wette, Phys. Rev. **179**, 873 (1969).
[14] S.M. Foiles and J.B. Adams, Phys. Rev. B **40**, 5909 (1989).
[15] G.D. Barrera, M.B. Taylor, N.L. Allan, T.H.K. Barron, L.N. Kantorovich, and W.C. Mackrodt, J. Chem. Phys. **107**, 4337 (1997).
[16] S. Biernacki and M. Scheffler, Phys. Rev. Lett. **63**, 290 (1989).
[17] P. Pavone, S. Baroni, and S. de Gironcoli, Phys. Rev. B **57**, 10 421 (1998).
[18] J. Xie, S. de Gironcoli, S. Baroni, and M. Scheffler, Phys. Rev. B **59**, 965 (1999); J. Xie, S.P. Chen, S. de Gironcoli, and S. Baroni, Philos. Mag. B **79**, 911 (1999).
[19] L. Kleinman and D.M. Bylander, Phys. Rev. Lett. **48**, 1425 (1982).
[20] D.R. Hamann, Phys. Rev. B **40**, 2980 (1989).
[21] X. Gonze, R. Stampf, and M. Scheffler, Phys. Rev. B **44**, 8503 (1991).
[22] D.M. Ceperley and B.J. Alder, Phys. Rev. Lett. **45**, 566 (1980); as paramerizted by J.P. Perdew and A. Zunger, Phys. Rev. B **23**, 5048 (1981).
[23] H.J. Monkhorst and J.D. Pack, Phys. Rev. B **13**, 5188 (1976).
[24] G. Lehmann and M. Taut, Phys. Status Solidi B **54**, 469 (1972).
[25] O. Madelung, W. von der Osten, and U. Rössler, in *Numerical Data and Functional Relationships in Science and Technology*, edited by O. Madelung, Landolt-Börnstein, New Series, Group III, Vol. 22, Pt. a (Springer-Verlag, Berlin, 1987).
[26] R.W. Lynch and H.G. Drickamer, J. Chem. Phys. **44**, 181 (1966).
[27] G.A. Slack and S.F. Bartram, Phys. Rev. B **46**, 89 (1975).
[28] G.H. Miller and T.J. Ahrens, Rev. Mod. Phys. **63**, 919 (1991).
[29] H.J. Mcskimin and P. Andreatch, Jr., J. Appl. Phys. **43**, 985 (1972).
[30] J.L. Warren, J.L. Yarnell, G. Dolling, and R.A. Cowley, Phys. Rev. **158**, 805 (1967); J.L. Warren, R.G. Wenzel, and J.L. Yarnell, in *Inelastic Scattering of Neutrons* (International Atomic Energy Agency, Vienna, 1965), Vol. I, p. 361.